Article Title
Tension during parametric excitation in submerged vertical taut tethers

Authors
Daniel Cantero
Anders Rønnquist
Arvid Naess

Manuscript version
Post-print = Final draft post-refereeing, before copy-editing by journal

DOI:
https://doi.org/10.1016/j.apor.2017.05.002

Reference:

Cantero, D., Rønnquist, A., Naess, A. (2017). Tension during parametric excitation in submerged vertical taut tethers. *Applied Ocean Research*, 65, pp. 279-289.

Title
Tension during parametric excitation in submerged vertical taut tethers

Authors
Daniel Cantero (1)
Anders Rønnquist (1)
Arvid Naess (1)

Affiliations
(1) Department of Structural Engineering, Norwegian University of Science & Technology NTNU, Trondheim, Norway

Abstract
The construction of a suspension bridge with floating pylons or a submerged floating tunnel requires the installation of a mooring system. The option of taut vertical tethers, similar to those used in tension-leg platforms, has been suggested in preliminary designs. The environmental loading on the tether, mainly due to wind waves and swell, results in a parametrically excited system. Certain loading conditions develop instabilities that translate into large horizontal motion. However, the effects of parametric resonance on the tension values have rarely been investigated. This paper aims to clarify the relation between lateral displacement and tether tension and to quantify the extreme tension values in the event of parametric resonance. The presented analysis is based on a full numerical model of the tether that includes geometric and hydrodynamic nonlinear effects. This model is used to investigate a representative example that illustrates parametric resonance and multiple parametric studies to assess the effects of the excitation frequency, amplitude, initial pretension, tether length and inclination angle on the tether's response. The results reported here provide the basis for a recommendation on designing a tether under parametric resonance regarding the ultimate extreme values and fatigue life.

Keywords
parametric excitation, instability, tether, tension, fatigue

1. Introduction

The National Roads Authority (NRA) in Norway is planning to cross several fjords along the west coast of the country as part of the "Ferry-free E39" project [1]. These crossings are characterized by large widths (up to 5 km) and depths (up to 1 km) that require unconventional engineering solutions. The preliminary designs suggest the construction of floating suspension bridges and submerged floating tunnels, as illustrated in Figure 1. A floating bridge is not a new idea and several examples can be found worldwide [2]. However, no precedent exists of a suspension bridge with multiple floating towers. A submerged floating tunnel is a structural concept that has been considered several times during the last century [3]; this tunnel essentially consists of a watertight buoyant tube at a certain depth underwater. To date, no such structure has ever been built. Both a long floating bridge and a submerged floating tunnel require a mooring system (Figure 1) to position these floating structures and to resist any imposed motion due to environmental loading. Since these structures would be located near the end of the fjord next to the sea, they would be exposed to sea states with wind waves and swell. In particular, swells have a long period and can last for several hours with effects that decrease linearly with water depth. There are concerns that

these environmental loads can parametrically excite the tethers of the mooring system, leading to parametric resonance or Mathieu instability.

a) b)

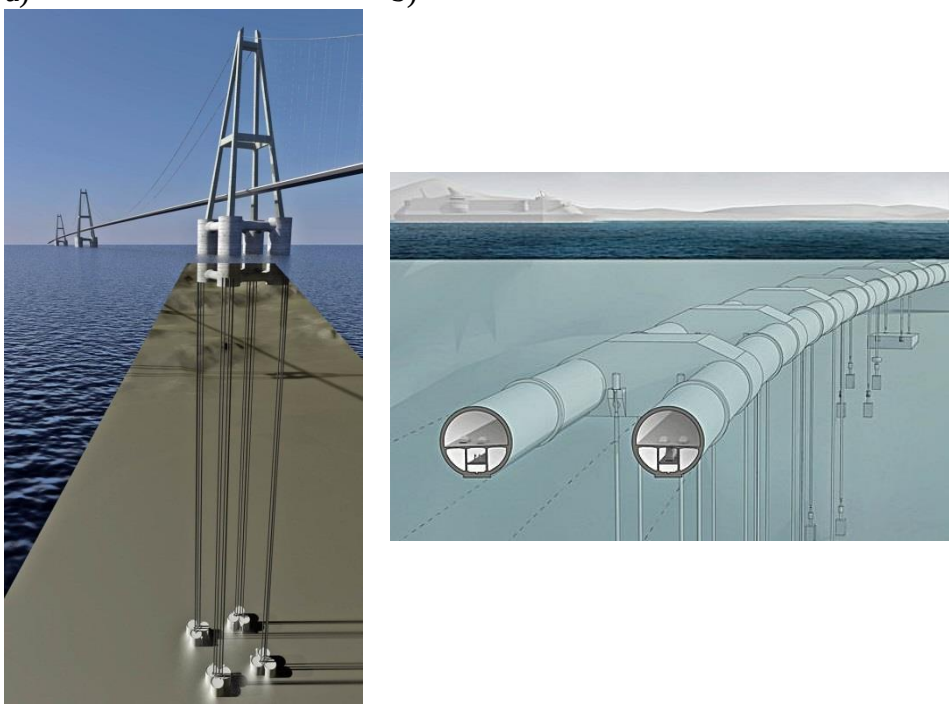

Figure 1: a) Floating cable-stayed bridge (Source: The Norwegian Public Roads Administration; https://flic.kr/p/pcgEt3); b) Submerged floating tunnel (Source: Snøhetta; https://flic.kr/p/yGeftB)

The taut mooring systems proposed in Figure 1 are similar to those used in Tension-Leg Platforms (TLP), which are usually made of steel tubes [4]. These tension pipes or tethers are designed to avoid slack cable configurations while also considering the peak and fatigue loading conditions [5]. As a result, these tethers have high pretension levels, zero net buoyancy and such massive dimensions that they cannot be considered to be compliant in the axial direction [4]. The environmental loads on the bridge towers or the submerged tunnel lead to varying tension levels and imposed motions on the tether that define a parametrically excited system.

A tether excited by harmonically varying imposed displacements of one of its ends is a parametrically excited system. Under certain conditions, parametric excitation leads to parametric resonance, which is an unstable situation that produces excessive lateral motion. The principal parametric resonance occurs when the frequency of the upper support motion is twice the fundamental frequency of the tether, i.e., a 2:1 frequency ratio. However, there are many more frequencies that induce instability in the system. Reasonably small amplitudes of anchorage oscillations may lead to important steady-state tether responses [6,7]. Furthermore, the greater the amplitude of the support motion is, the more frequencies there are that lead to unstable motion. Parametric excitation has been extensively studied in the field of differential equations and dynamic systems [8] and is generally described by the nonlinear Mathieu equation, where the excitation appears as time-varying coefficients. In bridge engineering, this phenomenon has been theoretically studied [6], investigated in laboratory experiments [7] and examined in cable-stayed bridges [9] where girder or mast oscillations have parametrically excited the stay cables.

The response of a submerged tether differs significantly to that of a dry tether because of the influence of hydrodynamic drag, which is the most important nonlinear contribution [10] and acts as an additional line damping component. Moreover, it has been shown [11,12] that the out-of-plane motion can be neglected when calculating the response of submerged slender structures. For a tether in an unstable condition, the quadratic fluid damping force limits the amplitude of the lateral motion [13]. An example of instability analysis for TLP tethers is given in [14]. Reference [15] derives an approximate analytical expression of tether displacements including hydrodynamic effects for principal parametric resonance. Additional literature reviews of the instabilities of risers and immersed slender structures can be found in [16,17].

The majority of the publications that have studied the parametric excitation of cables (either dry or submerged) mainly focus on lateral motion. As indicated in [18], tension has been overlooked in many studies. However, displacement is not the most important load effect. In fact, tension and stress values are of greater relevance when designing a taut mooring line. Some publications have specifically investigated tension to some extent. For example, reference [6] numerically shows how tension values develop on a dry cable during parametric excitation. In addition, [19] studies numerically tension using an experimentally validated model, while [18] shows that to achieve correct tension values, the model must account for spatiotemporal variations of tension along the cable. Moreover, [20] shows that the difference in magnitude (in spatial distribution) between the maximum and minimum tensions increases for a cable with significant sag. Furthermore, [21] concludes that the increase in pretension is ultimately equivalent to the increase in damping. In addition, [22] includes tension in the numerical analysis and states the need for understanding the impacts of parametric excitation. In [12], the dynamic tension values are measured for a submerged cable with sag in a scaled laboratory experiment, and recommendations are provided for the scaling and the support's boundary conditions. Other examples in the literature study the cable tension, but they do not consider the particular case of parametric excitation. For instance, [23] derives an approximate analytical expression of dynamic cable tension, and [24] obtains an analytical approximation of the probability distribution of the dynamic tension envelope for a random sea state. Therefore, even though some investigations have considered tether tension, additional studies are needed to characterize parametrically excited taut mooring systems.

Correct tether design should include the fatigue limit state [25] to avoid failure due to crack growth initiated from a welded joint in the tether. Detailed fatigue design recommendations can be found in [26]. The magnitude of the stress cycle and the number of load cycles are the key parameters that determine the accumulated fatigue damage of the studied member. However, based on the studies published to date, it is not possible to assess correctly the stress values of a taut mooring line with parametric resonance or its effects on the tether's fatigue life. The total stress in a tether is the combined result of several load effects, namely the axial load, bending moments and hydrostatic pressures. In most parts of the tether's length, the main contributor to the stress is the total (static + dynamic) tension, whereas bending moment has only a marginal effect [25]. On the other hand, bending moments can be very important near the tether ends. It is important to note, that this study does not evaluate all the aspects required for the design of a tether. The scope of this study is limited to the study of tension.

Therefore, the goal of this paper is to provide a clear description of parametric excitation on taut mooring lines with an emphasis on tension values; additionally, special attention is given

to extreme tether tension values. Very high cable tension could produce tether breakage, while very small or no tether tension could result in a momentarily slack member, which might induce large impulse forces on the moored structure when the cable becomes a taut line again. Moreover, a better understanding of the difference between the maximum and the minimum tension will allow us to suggest appropriate design procedures with respect to the tether's fatigue life. This paper also aims to clarify the relation between lateral displacement and tether tension in the event of parametric resonance. The presented analysis is based on a full numerical model of the tether that includes geometric and hydrodynamic nonlinear effects, which are difficult to include in an analytical study. In addition, realistic tether properties are used that are taken from preliminary designs of floating bridges and submerged floating tunnels.

The rest of the document starts with a description of the numerical model used in the study in Section 2. Then, based on the results from an example with a 2:1 frequency ratio, Section 3 clearly presents how parametric excitation originates and provides important comments on several aspects of the problem. Next (Section 4), a stability analysis for a wide range of frequency ratios and amplitudes is performed in terms of lateral displacements, total tension values and fatigue life calculations. The last section (Section 5) is a parametric study on three of the main design variables, namely, initial pretension, tether length and inclination angle.

2. Numerical model

Each tether of a mooring system can be modelled as a submerged beam. In addition, the wave loading on the bridge towers or the tube of the tunnel depends on the random sea state. However, due to the transfer function from wave action to structural movements, this random process leads to a narrow banded excitation of the mooring line [13,24]. Thus, the wave-induced motion is represented as a sinusoidal imposed vertical displacement of the upper beam support. Figure 2 shows a schematic representation of the tether and its support motion. Specifically, the numerical model is developed in ABAQUS [27] using 40 beam elements (B21) including nonlinear geometric effects. Each element consists of in-plane slender beam elements with two nodes and linear interpolation that translates to two degrees of freedom per node The type and number of elements was decided based on a convergence study (not reported here) that ensured accuracy and stability of the numerical results. Since large deformations are expected in the model, equilibrium is formulated in the deformed state, i.e. considering nonlinear geometric effects. The same configuration is used throughout this study. The contribution of the hydrodynamic effects (drag and added mass) is represented by the Morison equation using the Aqua toolbox in ABAQUS. A beam of total length L is assumed to have an initial pretension T_0 and supports that are free to rotate (pin), while the upper support also follows a prescribed motion. The fundamental frequency f_1 is calculated considering the beam's self-weight and the added mass contribution of the surrounding water. The imposed cyclic motion of the upper support is defined by its amplitude A and frequency f. This numerical model is used to calculate the displacement and tension of several points of interest along the tether's length. This analysis in ABAQUS was done with a direct numerical integration of the equations of motions, in order to correctly account for the nonlinear effects.

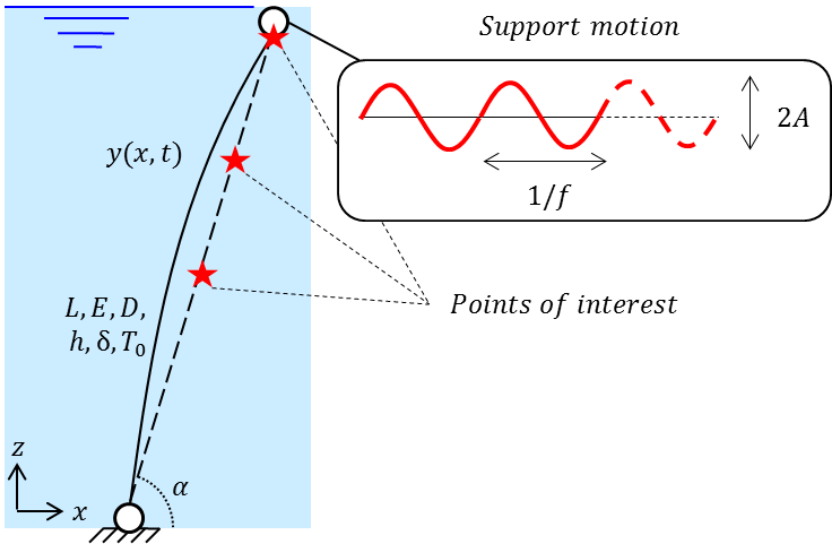

Figure 2: Sketch of tether and support motion

The particular tether properties used in this study are listed in Table 1 and are used throughout the paper unless otherwise specified in the text. The values in Table 1 correspond to those suggested in the preliminary design of the mooring system for the floating bridge and submerged tunnel of the Bjørnafjord crossing, which is part of the "Ferry-free E39" project [1]. Moreover, similar tether dimensions and pretensions can be found in [14,25,28]. To correctly account for the hydrodynamic effects, two important parameters are needed, namely, the added mass coefficient C_A and the drag coefficient C_D. The numerical values of these coefficients are listed in Table 1 and they are taken from the recommendations in [29]. Furthermore, a small internal damping of only 0.1% is assumed to avoid any spurious numerical effects. Mooring system damping is difficult to assess precisely [30], but a higher internal damping can be expected. Therefore, the results presented here can be considered conservative. In the numerical simulation, 120 loading cycles of the upper support motion are computed for every simulated case presented here; this is more than sufficient for developing parametric resonance and/or reaching a steady-state situation. The numerical time integration of the solution is performed using a sufficiently small time step that gives a minimum sampling rate of 100 Hz. The numerical stability and accuracy of the solution was assessed in a preliminary convergence study that is not shown here.

Table 1: Tether properties

Description	Symbol	Value	Unit
Length	L	400	m
Young's modulus	E	$2.1 \cdot 10^{11}$	N/m^2
Diameter	D	1.119	m
Thickness	h	38	mm
Density	δ	7800	kg/m^3
Initial pretension	T_0	$18.5 \cdot 10^6$	N
Inclination angle	α	90	degrees
Fundamental frequency	f_1	0.1299	Hz
2nd frequency	f_2	0.2648	Hz
3rd frequency	f_3	0.4096	Hz
Added mass coefficient	C_A	1	-
Drag coefficient	C_D	1.5	-

3. Tension during parametric excitation

This section aims to clarify what parametric excitation is based on a particular example that features a frequency ratio (support motion frequency f to tether's fundamental f_1) of 2:1. Special attention is given to the tension values and their relation with the lateral displacements of the tether. The numerical model presented in Section 2 is computed for the tether with the properties listed in Table 1. The results from the example considered in this section are dissected to examine different aspects of the problem in detail, which are each presented in a different subsection. First, the influence of hydrodynamic effects is assessed by comparing the response of a dry tether to a submerged tether. Then, the parametric excitation phenomenology is explained graphically, providing clear insight into why instability occurs. In addition, the following subsections discuss the spatial distribution of the tension values, how to define a stability criterion and the definition of dynamic factors to assess the magnitude of extreme tension values.

3.1 Dry tether

A tether modelled as a linear system and parametrically excited at a critical frequency has an unbounded solution. The result is the classic parametric resonance of the linear Mathieu equation featuring exponential growth. In a truly linear system, the amplitude increases until the system is destroyed [8]. However, real physical systems do not exhibit unbounded responses. By including the nonlinear effects, a more realistic model is obtained. During parametric resonance, the nonlinearities limit the oscillation amplitudes. Therefore, the tether is modelled to include nonlinear geometric effects. Figure 3a shows the time-history of the mid-span lateral displacements, which exhibit exponential growth over time until a certain maximum (or minimum) value is reached. Then, the displacements decay and repeat the exponential growth again. For this particular example, the maximum displacement is 4.47 m, while the amplitude of the upper support motion is only 0.10 m. This beating-like behaviour during parametric resonance is also reported in [6,15,20].

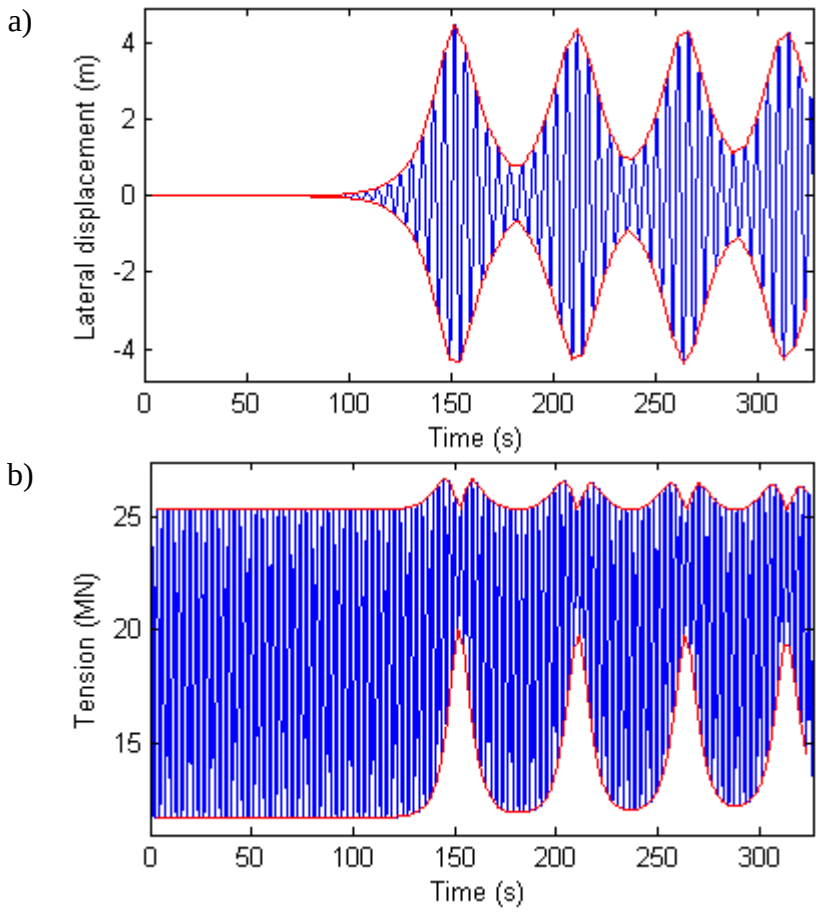

Figure 3: Dry tether response at the mid-span for a 2:1 frequency ratio: a) Horizontal displacement; b) Total tension (red lines = outer envelopes to response)

Intuition suggests that the internal tether tension should have a similar evolution over time or should at least feature some extreme values at the same times as those reported for the displacements in Figure 3a; however, this is not the case. Figure 3b shows the time-history of the total tension at the upper support. Before instability is triggered, the tension values oscillate according to the imposed motion of the support. After parametric resonance has started, both the maximum tension values and the minimum tension values increase. Moreover, the difference between the tension extremes is lowest exactly when the maximum displacements occur. This counterintuitive behaviour of the tension was also reported in [6] and explained as the synchronous compensation of the tension oscillations by the support motions.

3.2 Submerged tether

As mentioned in the introduction, the hydrodynamic effects are the greatest contributors to the damping of the system. Parametric resonance of the submerged tether can still occur, but the displacement and tension responses differ significantly. The time-history response of the lateral displacement is given in Figure 4a, which also includes the hydrodynamic effects. The figure shows that the lateral displacement of the tether starts to increase rapidly after 100 s of excitation and reaches steady-state conditions after 220 s. This increase is mainly limited by the dissipative effects of the hydrodynamic contributions. The extreme lateral displacement values at mid-span are indicated by the labels $u_{x,max}^{mid}$ and $u_{x,min}^{mid}$. For reference, the figure shows the amplitude of the vertical motion (±0.1 m) of the upper support in dashed black

lines; in addition, the envelopes of the time series are indicated with a solid red line. Parametric resonance plays an important role in the rapid growth. However, compared to the dry tether example (Section 3.1), the extreme displacements only reach 0.55 m, and more interestingly, no beating phenomenon is observed. These differences between dry tether (Figure 3a) and submerged tether (Figure 4a) can only be attributed to the additional damping of the hydrodynamic effects.

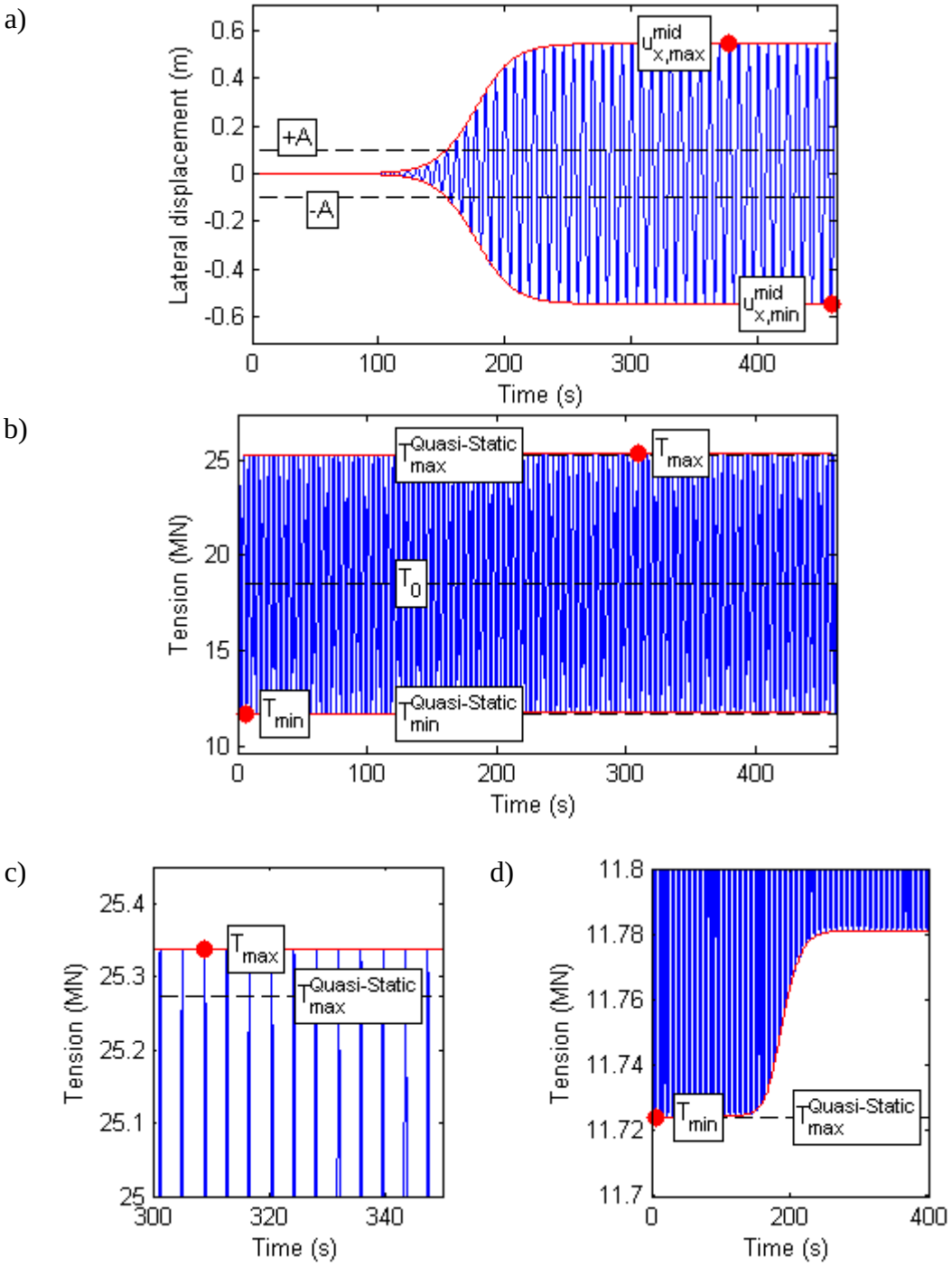

Figure 4: Submerged tether response at the mid-span for a 2:1 frequency ratio: a) Horizontal displacement; b) Total tension; c) Zoomed view near T_{max}; d) Zoomed view near T_{min} (red lines = outer envelopes to response)

Figure 4b presents the total tension of the submerged tether at the mid-span; this figure shows that the tension values are barely affected by the parametric resonance. For reference, the initial tether tension T_0 is indicated in the figure. The horizontal dashed black lines labelled $T_{max}^{Quasi-Static}$ and $T_{min}^{Quasi-Static}$ reveal the extreme quasi-static tension values expected due to the imposed cyclic motion ($A = 0.1\ m$). While the system response is stable ($t < 100\ s$), the tension values oscillate following the expected quasi-static response due to the imposed motion. However, when parametric resonance starts, only a small change can be observed. Then, the maximum tension values slowly increase to T_{max}, which is only slightly greater than $T_{max}^{Quasi-Static}$ (Figure 4c). On the other hand, the minimum tension value T_{min} occurs at the beginning of the time series because the minimum tension values actually increase over time, even if only marginally (Figure 4d). Therefore, the effect of parametric excitation on the dynamic tension is very small. This result is somewhat counterintuitive: a situation that has large lateral motion (Figure 4a) features only very small dynamic tension effects (Figure 4b). This can be explained analysing the lateral displacement response. Even though the parametric resonance has been triggered, the steady-state response features constant amplitude due to the energy dissipation effects of the hydrodynamic contribution. In addition, this amplitude is an order of magnitude smaller for the submerged tether (Figure 4a), compared to the dry example in Figure 3a. These smaller and stationary lateral motions are not big enough to induce significant changes in the tension variation compared to the quasi-static response (Figure 4b).

3.3 Phenomenology

To better understand parametric excitation, the response of the tether can be illustrated using a 3D graphical representation. The time-histories of the horizontal displacement at mid-span (u_x^{mid}) and the vertical motion at the upper support (u_y^{upper}) are plotted together in Figure 5 for the 2:1 frequency ratio example. Both displacements are presented at the same scale to clearly visualize the large magnification observed during parametric resonance. Here, the colour code is proportional to the system's energy content, where blue values indicate low energy levels and red values indicate high energy levels. Figure 5 shows only the part of the response that has a rapid growth due to parametric instability. First, due to the boundary condition motion, only vertical displacements with small energy values are observed. However, as soon as the parametric resonance is triggered, the horizontal displacements quickly increase to several times greater than the imposed vertical motion. While the vertical motion ranges between ±0.1 m, the lateral displacement ranges between ±0.5 m.

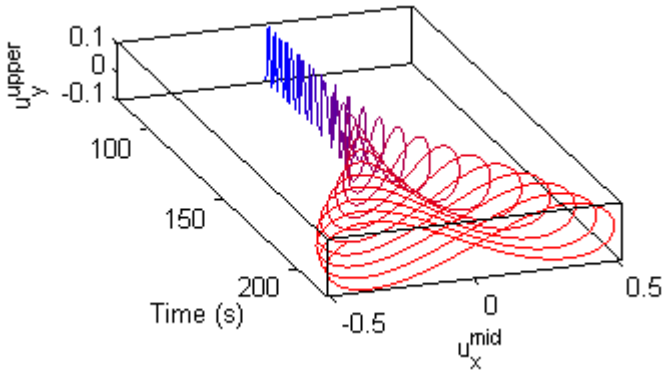

Figure 5: 3D plot of the tether response at the mid-span

The physical explanation of why the lateral displacements of the tether increase so much is illustrated in Figure 6. The figure shows several instances (A-E) of one full cycle of the tether's lateral motion. Because of the 2:1 frequency ratio, during a single cycle, the upper support moves vertically two full cycles. Every time that the tether is fully bent and is returning to its static equilibrium position (instances A, C and, E in Figure 6), the upper support is moving upwards. This positive vertical movement makes the tether move faster. For every repetition of this cycle, the imposed motion adds more energy to the system until it eventually becomes unstable. Section 4 shows that other frequency ratios can also lead to unstable responses, and that the instability mechanism for those cases is similar to the one presented in Figure 6. However, the 2:1 frequency ratio provides the most intuitive example and reaches instability more quickly (requires fewer cycles); therefore, this example is generally called principal parametric resonance.

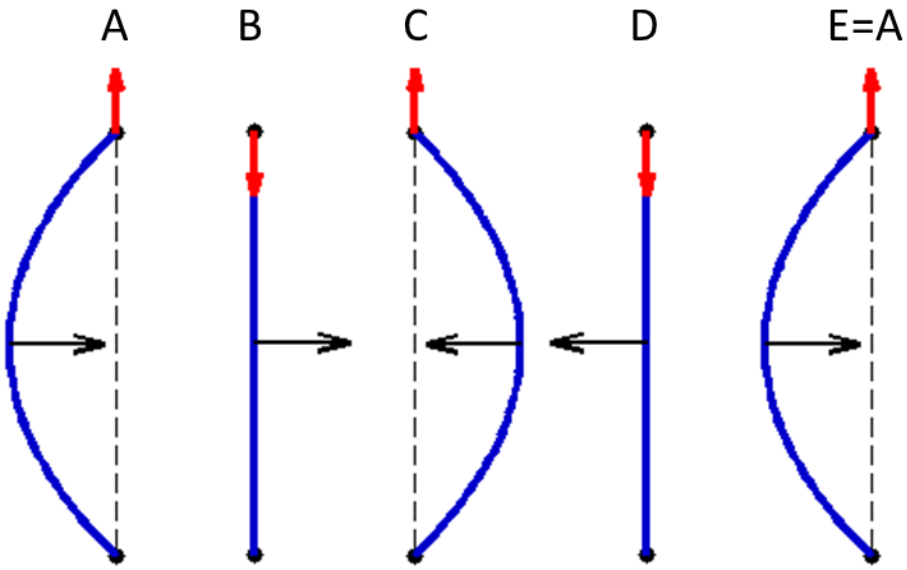

Figure 6: Multiple instances of one full cycle of tether lateral displacement for the 2:1 frequency ratio (blue lines = tether lateral deformation; black dashed lines = static equilibrium position; black horizontal arrow = direction of movement; and red vertical arrow = imposed vertical motion)

3.4 Spatial distribution

Because of the contribution of higher modes of vibration, it can be argued that extreme load effects can be found anywhere along the tether. Generally, the maximum lateral displacement occurs at the mid-span, but this is not necessarily always the case. For instance, an ideal situation that excites only the 2nd mode of the tether would lead to maximum motion at the quarter-span, while the mid-span section featured no lateral vibration. For this reason, every simulation in this study calculates the response of several points of interest along the tether length. The conclusions are based on the simultaneous analysis of multiple locations, thus including the effects of higher vibration modes.

As noted in the introduction, to correctly evaluate the total tension, it is important to consider its spatial distribution along the tether, as verified by the results obtained for the 2:1 frequency ratio example. The tension time-histories for all the elements in the model are extracted, and Figure 7 shows the instantaneous maximum and minimum tension values

along the tether in two separate curves. In other words, Figure 7 shows the envelope of maximum and minimum tension along the tether. At the beginning of the simulation (Figure 7a), some differences exist between the extreme values during the initial transient vibration phase because the sudden application of the imposed motion at the upper support produces additional vibrations that travel as compressive waves but vanish rapidly. In the remaining duration of the example, the maximum and minimum tension values anywhere along the tether are practically identical. This is also true when parametric resonance occurs and the system has reached its steady-state response (Figure 7b). This indicates that tension is constant along the tether length at any given time instant. Nevertheless, in subsequent simulations, a range of selected points of interest along the tether length is examined, similar to the lateral displacement.

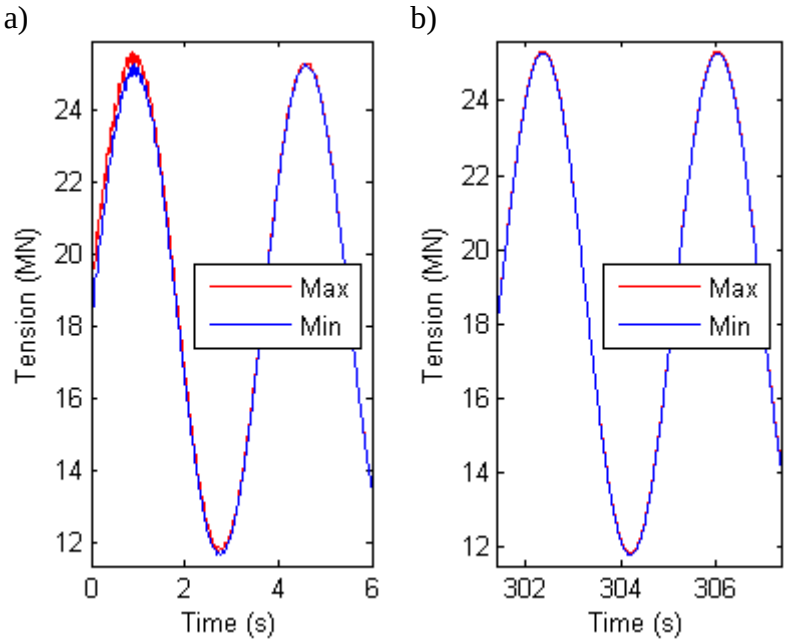

Figure 7: Instantaneous maximum and minimum tension along the tether during: a) Initial transient vibration; b) Parametric resonance

3.5 Stability criteria

In parametric excitation studies, identifying when the system is unstable or has reached parametric resonance is of paramount importance. In theoretical studies that work directly on a mathematical description of the problem, instability can be defined as a mathematical condition [8]. However, when dealing with measurements or, as in this study, with simulated results, it is not trivial to clearly flag instability, and procedures to do so are generally not well documented. One possibility is using the Lyapunov exponents [31], as reported in [32] and [33]; however, in practice, this is not without problems and it can be computationally time consuming. Therefore, this study uses a ratio based on the Root Mean Square (RMS) values of the response. For instance, the horizontal displacement response of the tether in Figure 4a corresponds to an unstable situation. A convenient way to identify instability is by comparing the RMS (proportional to the energy content) of the signal to the RMS of the first few cycles. Ratios close to one indicate that the dynamic behaviour has not changed considerable and that the response is stable. However, as the RMS ratio increases, the system can be considered unstable. This definition of stability in relative terms allows us to easily apply the criterion to any point along the tether without previous knowledge of its expected stable behaviour. Here, the stability criterion is defined for a RMS ratio > 1.1 to allow for

small spurious increases that do not correspond to instability. For the particular case shown in Figure 4a, comparing the last four cycles to the first four cycles of the response gives a ratio of 10.73.

3.6 Extremes evaluation

To characterize the effects of parametric resonance on the total tension values of the tether, it is necessary to quantify both extremes, i.e., maximum and minimum tension values, which are convenient to analyse in terms of dynamic factors. Here, we introduce the Dynamic Amplification Factor (*DAF*) and the Dynamic Reduction Factor (*DRF*), which are defined in Eq. (1) and Eq. (2) respectively using the notation presented in Figure 4b. In essence, these factors are the normalizations of the dynamic tension increments with respect to the quasi-static tension increments due to the imposed upper support motions. For the particular case shown in Figure 4b, *DAF* is 1.0094, which means that the quasi-static increment $\Delta T_{max}^{Quasi-Static}$ has to be increased by only 0.94% to account for the dynamic effects. On the other hand, *DRF* is 0.9923, which is equivalent to decreasing $\Delta T_{min}^{Quasi-Static}$ by 0.77%. Values of *DRF* that are less than one indicate that the total minimum tension is larger than the quasi-static minimum, as shown in Figure 4b.

$$DAF = \frac{\Delta T_{max}}{\Delta T_{max}^{Quasi-Static}} = \frac{T_{max} - T_0}{T_{max}^{Quasi-Static} - T_0} \quad \text{Eq. (1)}$$

$$DRF = \frac{\Delta T_{min}}{\Delta T_{min}^{Quasi-Static}} = \frac{T_{min} - T_0}{T_{min}^{Quasi-Static} - T_0} \quad \text{Eq. (2)}$$

4. Stability study and fatigue

So far, this paper has presented results for a particular example where the imposed support motion has a 2:1 frequency ratio and a specific amplitude (0.1 m). However, in addition to occurring for multiple frequency ratios, parametric resonance is also strongly dependent on the amplitude of the imposed motion. Therefore, this section performs stability analysis for a wide range of frequency ratios (f/f_1) and amplitudes (A) of the upper support motion. In particular, the frequency ratio is varied in a discrete space from 0.25 to 3.5 in increments of 0.05, while the amplitude varies from 0.005 m to 0.1 m in 0.005 m increments, providing a total of 1320 simulated cases. The stability is studied first in terms of lateral displacement, then it is compared to the results of tether tension and finally the consequences on fatigue life calculation are evaluated.

4.1 Lateral displacement

Figure 8a shows the instability diagram based on the lateral displacement of the tether at the mid-span. Each of the studied f/f_1 and A combinations is represented as a dot. If the particular case renders a stable solution, it is depicted as a small black dot; when the combination leads to an unstable result, it is represented by a larger dot. As expected, the results clearly feature distinct areas with parametric resonance, which are usually called instability tongues. The biggest tongue emanates from the 2:1 frequency ratio and corresponds to the principal parametric resonance. In addition, several other tongues correspond to other frequency ratios, higher vibration modes and/or a combination of

harmonics. Figure 8a also shows the theoretical tongues associated to the Mathieu equation. These theoretical instability regions are drawn based on the analytical expressions reported in the Appendix. These analytical expressions derive from the theoretical analysis of a taut simply supported cable using the harmonic balance method considering two harmonic terms. The direct comparison of the numerical and theoretical instability regions shows a good agreement.

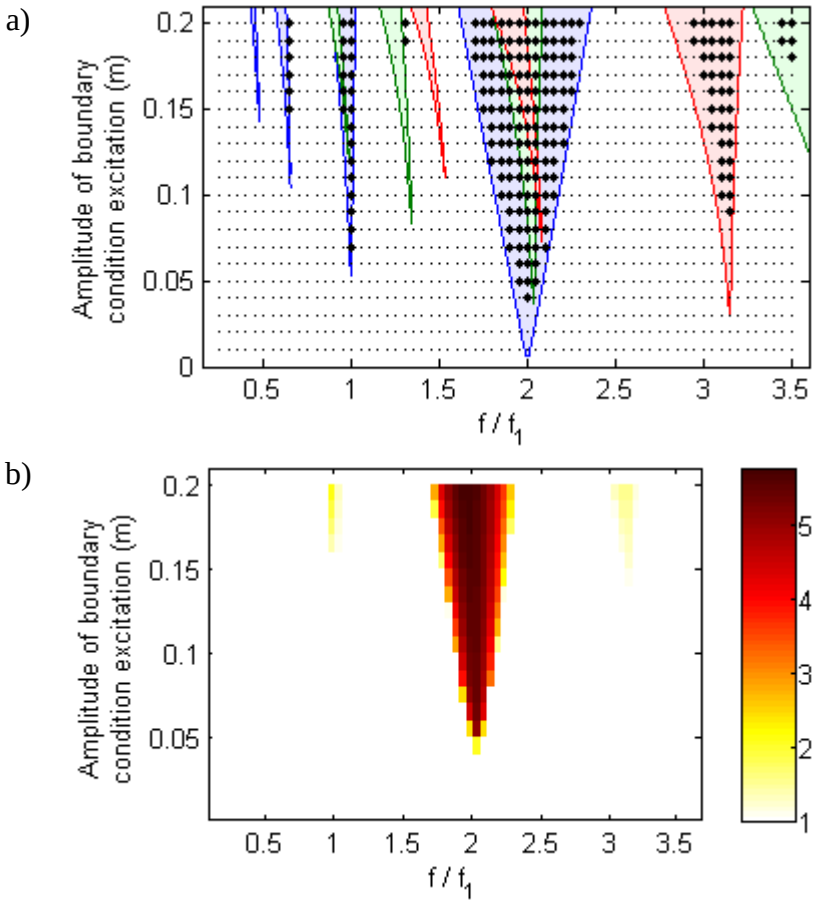

Figure 8: a) Instability map for numerical results (stable = small dot, unstable = large dot) and theoretical instability tongues (see Appendix) associated to tether's 1st mode (Blue), 2nd mode (Green) and 3rd (Red) mode; b) Normalized lateral displacement values

Figure 8a is the standard stability map, which is also called a Strut diagram. This map allows us to clearly identify the instability regions of the problem. However, it is difficult to assess the relative importance of each of the tongues. In theory, for infinitely long excitations, all unstable cases will reach steady-state and similar extreme displacement values. However, in practice, it is interesting to examine the maximum displacements achieved during parametric resonance for a finite duration of excitation. Figure 8b shows the maximum lateral displacements normalized by the amplitude of the support motion. In all the simulated cases, the excitation lasted for 120 cycles. The results clearly show that the 2:1 frequency ratio tongue has the highest values, indicating a quicker instability and confirming its importance compared to the other tongues.

4.2 Tether tension

The effect of tether instability is evaluated in Figure 9 for the extreme tension values in terms of the dynamic factors *DAF* and *DRF* defined in Section 3.6. There is a clear correlation between the instability tongues shown in Figure 8 and the results in Figure 9. However, the actual numerical values of the factors are remarkably small. In the case of *DAF* in Figure 9a, the overall maximum value is 1.019, meaning that the maximum total tension (static + dynamic) is only 1.9% greater than that in the static case. The results in Figure 9b show that the minimum tension in the tether is either equal to or slightly less than the minimum static tension. In particular, the absolute minimum *DRF* value is 0.977, which corresponds to a 2.3% decrease in the static tension.

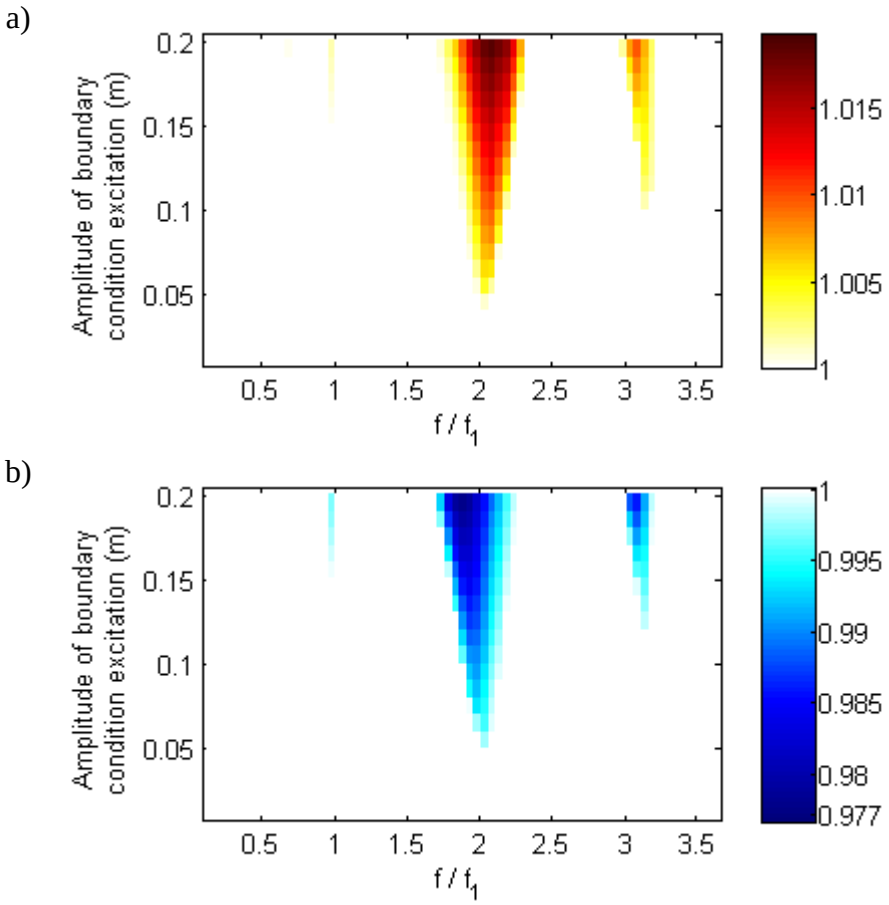

Figure 9: Tension dynamic factors: a) *DAF*; b) *DRF*

The main conclusion drawn from the results in Figure 9 is that the dynamic tension contribution during parametric resonance is very small. It is also interesting to note that outside of the instability tongues, the dynamic factors are virtually equal to one. In other words, the total tension during stable conditions is the same as the total tension due to quasi-static loading. Therefore, if the design of a tether is based on a maximum displacement criterion, the results in Figure 8 suggest that any possibility of parametric resonance should be avoided. However, in reality, a tether is designed with respect to the maximum stress levels. According to the results in Figure 9, the extreme tension levels are either close to or identical to the tension based on a quasi-static response, indicating that the dynamic effects of parametric resonance are very small. Furthermore, this conclusion can be refined when directly exploring the consequences on fatigue calculations.

4.3 Fatigue

This section evaluates the effect of parametric excitation on the fatigue life calculations of tethers by introducing a new factor that facilities this analysis. The main parameter in any fatigue calculation is the stress range *S*; this range is directly proportional to the tension increment ΔT, which can be written as:

$$\Delta T = T_{max} - T_{min} \quad \text{Eq. (3)}$$

Using the definitions of *DAF* and *DRF* given in Eq. (1) and Eq. (2):

$$\Delta T = DAF \cdot \Delta T_{max}^{Quasi-Static} - DRF \cdot \Delta T_{min}^{Quasi-Static} \quad \text{Eq. (4)}$$

In the case of taut tethers, it can generally be assumed that the static tension increment (ΔT_{max}^{Static}) due to positive vertical displacement of the support is of the same magnitude but opposite sign as the static tension increment (ΔT_{min}^{Static}) due to lowering the support motion. Thus, representing both tension increments as $\frac{1}{2}\Delta T^{Static}$, we can rewrite expression Eq. (4) as:

$$\Delta T = \frac{(DAF + DRF)}{2} \cdot \Delta T^{Quasi-Static} = DF \cdot \Delta T^{Quasi-Static} \quad \text{Eq. (5)}$$

Eq. (5) introduces the Dynamic Factor (*DF*) and can be used to easily determine the total tension increment (including static and dynamic effects) by simply factoring the tension increment obtained from quasi-static analysis. Moreover, *DF* is the average of the *DAF* and *DRF* values. Figure 10 gives the numerical values of this new factor for the same frequency ratios and amplitudes studied in the previous subsections. Similarly, the results show the presence of multiple instability tongues, and the tongue emerging near the 2:1 frequency ratio shows the highest values. In particular, the maximum value in Figure 10 is 1.006, and the minimum value is 0.987, which are equivalent to 0.6% and -1.3% changes in the tension increment, respectively. The *DF* values for a given critical frequency ratio (say 2:1) may be either negative or positive depending on its excitation frequency with respect to the centre of the corresponding instability tongue. Therefore, the stress range *S* obtained from a quasi-static analysis should be decreased or increased, effectively increasing or decreasing the calculated fatigue life of the member, respectively. However, the *DF* values are very small regardless of their sign, which supports the assertion that it is safe to perform only quasi-static simulations for the fatigue calculations of a tether. Even if parametric resonance occurs, the dynamic effects on tension are sufficiently small to be covered by the general safety factors of the design process.

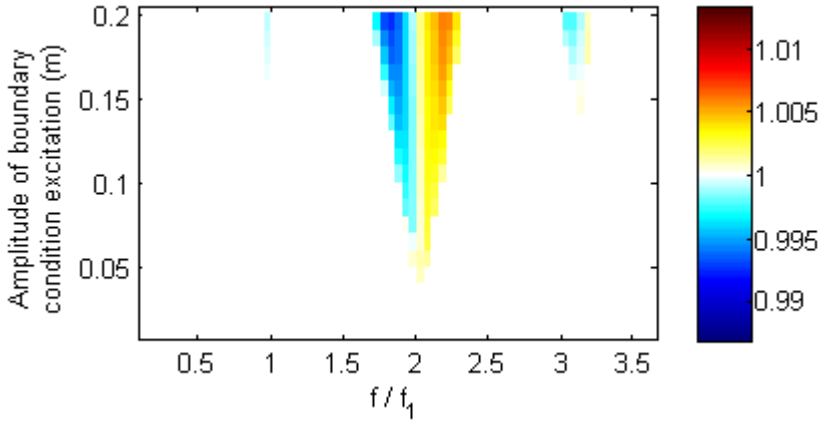

Figure 10: Tension Dynamic Factor (*DF*)

5. Parametric studies

The tether properties used in the previous sections and listed in Table 1 correspond to a representative example of the tethers to be used in the construction of a floating bridge and a submerged floating tunnel. However, these properties are derived from preliminary designs, and some variations can be expected. This section evaluates the influence of three of the main design variables faced in the project. In particular, the following subsections investigate the effect of the initial pretension, tether length and inclination angle. The studies evaluate their influence on system stability and, most importantly, its effect on the total tension. For these analyses, the frequency ratio is set to 2:1, and the amplitude A is 0.1 m. The fundamental frequency of the tether changes in each study and needs to be recalculated for each new tether configuration.

5.1 Pretension

The influence of pretension is first evaluated in terms of the normalized mid-span tether displacement in Figure 11a, which clearly shows a decrease with increasing pretension. That is, the system's stability increases with increasing pretension. This fact is also shown as an increase in the number of cycles needed to trigger parametric resonance, as plotted in Figure 11b. Similarly, the dynamic factors that quantify extreme tension increments (*DAF* for maximum and *DRF* for minimum) also decrease with increasing pretension. Nevertheless, the numerical values of these factors are still quite small. Even for the lowest pretension level, tension increases of less than ±3% need to be accounted for. For the *DF* values, the dynamic factor for fatigue calculations remains constant and very close to one, which confirms that the quasi-static calculation is sufficient for any of the considered pretension levels.

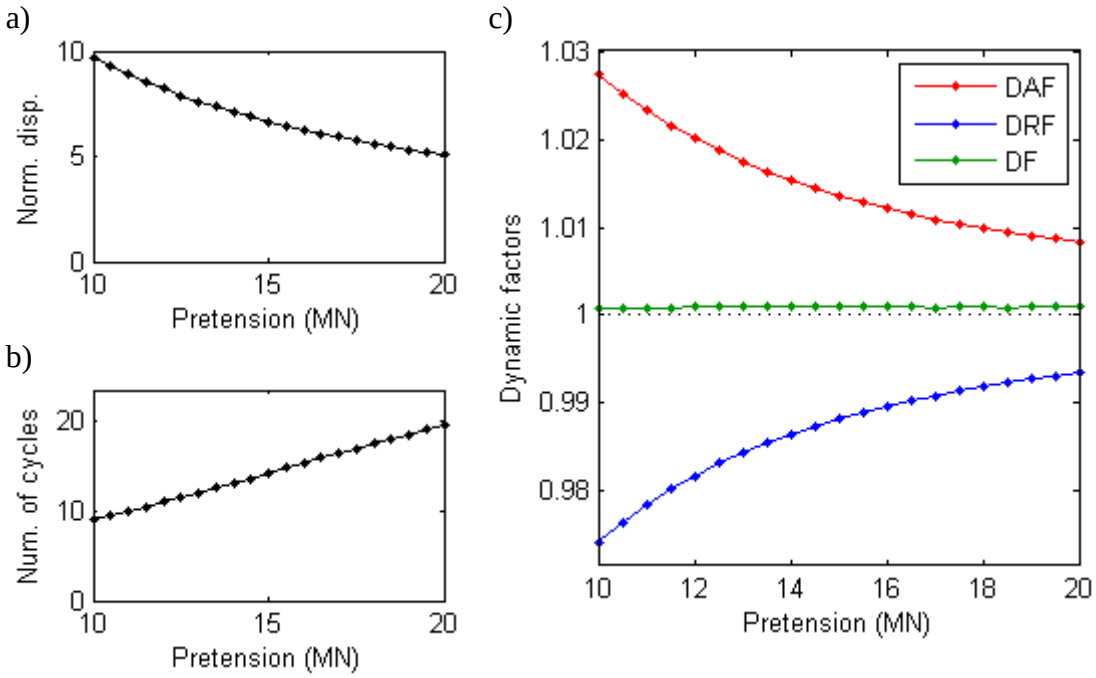

Figure 11: Influence of pretension: a) Normalized lateral displacement at mid-span; b) Number of cycles to initiate parametric resonance; c) Dynamic factors

5.2 Length

The length of the tether clearly depends on the depth of the seabed. The distance between the floating construction (either bridge tower or submerged tunnel) and the anchoring point of the mooring line varies significantly along the length of the structure. This study evaluates the influence of parametric resonance on tethers with different lengths. All the cases are simulated for a support motion with the same amplitude of 0.1 m. Thus, the extreme static tension values are greater for shorter tether lengths (Figure 12a) because the elastic stiffness of the system is inversely proportional to the length. In other words, shorter tethers are stiffer and lead to greater tension values for the same imposed support motion. As a result, the higher quasi-static tension oscillations observed in shorter tethers lead to instabilities with larger lateral displacements, as shown in Figure 12b. Similarly, the extreme total tension values also increase (or decrease) for shorter tethers (Figure 12c). However, as observed throughout this paper, these dynamic factors are remarkably small. In this case, only ±5% tension variations are expected for the shortest mooring line. Nevertheless, the dynamic factor for fatigue *DF* remains nearly constant and can be approximated as equal to one.

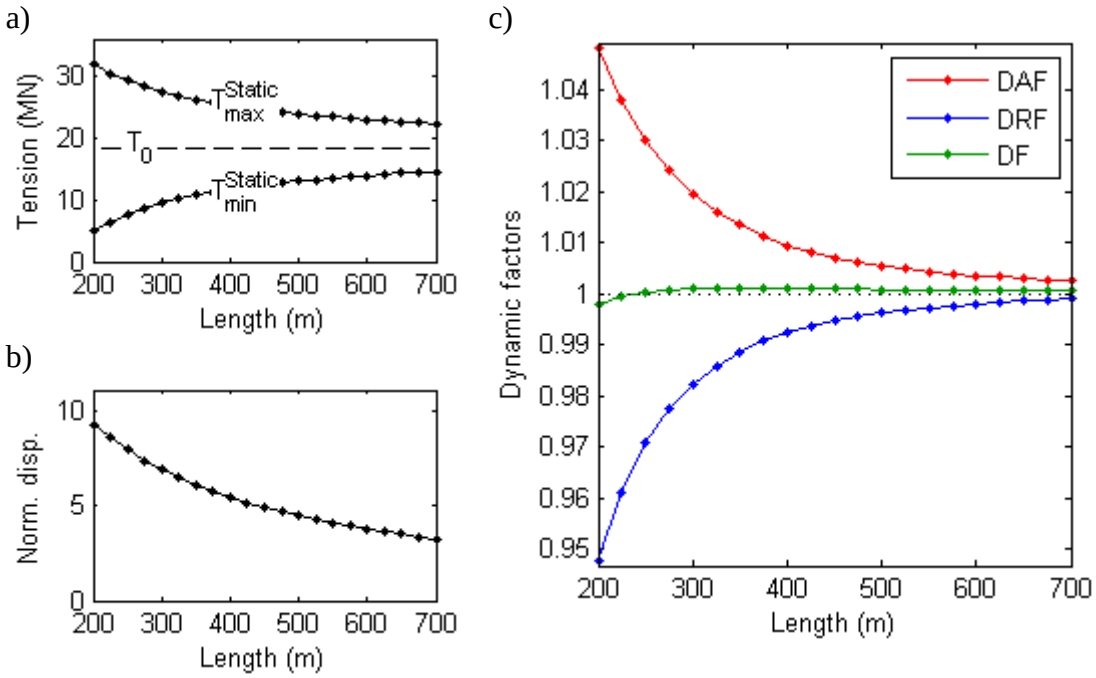

Figure 12: Influence of tether length: a) Static tension values; b) Normalized lateral displacement at mid-span; c) Dynamic factors

5.3 Inclination angle

A vertical mooring system such as the one investigated in this study so far imposes little or no restraint in the horizontal plane. Therefore, large lateral motions could be induced if the floating structure is too flexible or the lateral loading is sufficiently strong. One possibility for providing additional lateral stiffness is to include pairs of inclined mooring lines in opposite configurations. This study assesses the impact of the tether inclination angle on the system's stability. According to the definitions in Section 2, an angle of 90° corresponds to a vertical mooring line. Figure 13a shows the tether response in terms of the normalized horizontal displacement. Smaller angles are shown to give a stable response, while angles closer to vertical feature instability. This finding is supported by the results in Figure 13b that show the number of cycles needed to trigger parametric resonance. For configurations with small inclination angles, no results are shown because the parametric resonance is not triggered. In general, stability increases with a decreasing inclination angle; this can be explained by the combination of two effects. First, the actual tether length increases at smaller angles, which leads to greater system stability, as shown in Section 5.2. Second, the imposed vertical motion is effectively divided into two parts, namely, the perpendicular and tangential components. Only the tangential component parametrically excites the system, which decreases with decreasing inclination angle. The perpendicular component produces a normal external load and has a much smaller effect on the dynamics of the tether. Finally, Figure 13c shows the effect of tether inclination on the total tension dynamic factors. The stability of the system greatly influences the numerical values of the factors, obtaining higher (or lower) values in the event of unstable configurations. However, and in accordance with the previous results, the actual numerical values are very small. In this case, all the results indicate reductions smaller than ±1% compared to the static solution.

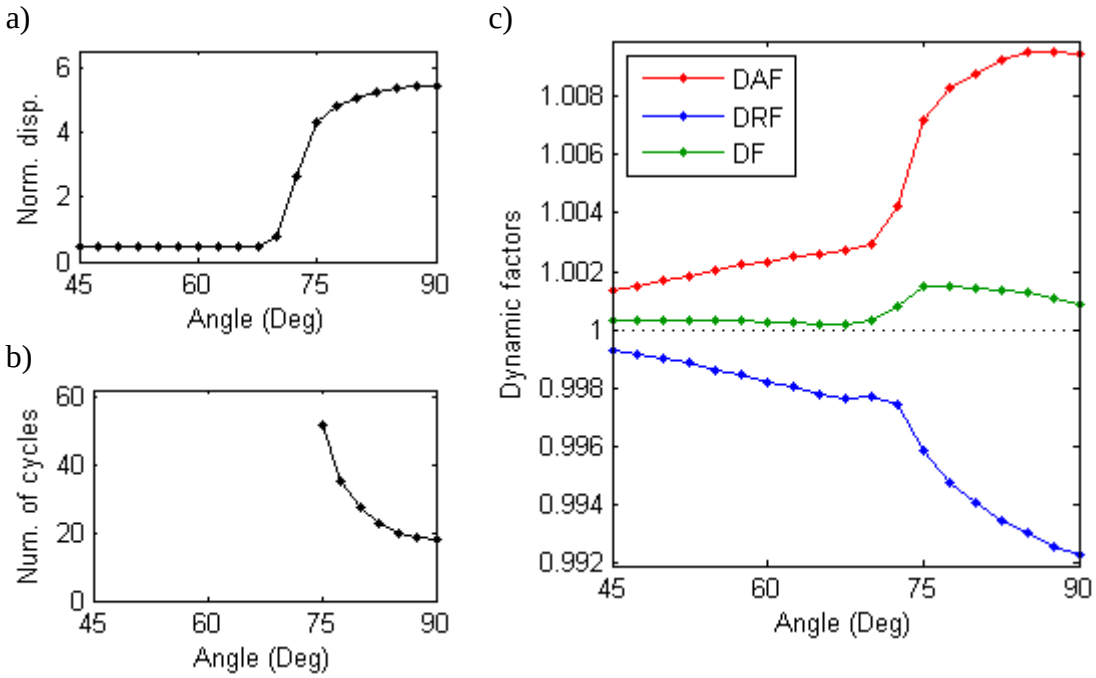

Figure 13: Influence of tether inclination: a) Normalized lateral displacement at mid-span; b) Number of cycles to initiate parametric resonance; c) Dynamic factors

Conclusions

This document has investigated the effect of parametric excitation on the response of taut mooring lines. Particular emphasis is given to the total tension values in the tether. The analysis is done using a nonlinear numerical model of a tether based on preliminary designs of floating bridges and submerged floating tunnels. The results from a 2:1 frequency ratio example show that the tension values are barely affected by the parametric resonance. This outcome is somewhat counterintuitive, indicating that unstable situations with large lateral motions feature very small dynamic tension effects. This conclusion is also confirmed by an investigation that considers a wide range of frequency ratios and amplitudes. Despite the clear correlation between instability tongues (due to lateral displacements) and extreme total tension values, the actual increment in tension due to parametric resonance is remarkably small. The results are expressed in terms of dynamic factors to evaluate the extreme (maximum and minimum) tension values and the effects on the fatigue life calculations. For stable configurations, the total tension can be correctly approximated using a quasi-static analysis. On the other hand, during parametric resonance, the dynamic effects are generally small and can be regarded as negligible. Therefore, if the design of a tether is based on the extreme tension levels, this study repeatedly shows that no dynamic analysis is needed to account for the effects of parametric resonance. Instead, a quasi-static response due to the expected vertical motion of the support is sufficiently accurate. This is applicable for calculating the extreme tension values in an ultimate limit state analysis as well as for the stress range and cycle counting needed in a fatigue limit state analysis.

Appendix. Analytical expressions of transition curves

This appendix provides the analytical expressions of the transition curves for a taut cable parametrically excited by inline harmonic support motion. Note that the final expressions reported here correspond to adapted and improved versions of the equations published by the authors in [34], where additional details on the derivation can be found. In particular, the

derivation outlined below corresponds to a simply supported cable of length L, with an initial axial force N and a support motion $\Delta x(t) = A\cos(\Omega t)$, where A is the amplitude and Ω is the frequency of the motion. The lateral displacements $u(x,t)$ of such a cable can be described by the equation of motion Eq. (A1), where m and c are respectively the mass and viscous damping per unit length and $\Delta N(t)$ is the variation of the axial force due to the support motion.

$$m\frac{\partial^2 u}{\partial t^2} + c\frac{\partial u}{\partial t} - \big(N + \Delta N(t)\big)\frac{\partial^2 u}{\partial x^2} = 0 \qquad \text{Eq. (A1)}$$

The solution can be expressed as the sum of n modes of vibration Φ_j factored by the generalized coordinates U_j:

$$u(x,t) = \sum_{j=1}^{n} U_j(t)\phi_j(x); \qquad \phi_j(x) = \sin\left(\frac{j\pi x}{L}\right) \qquad \text{Eq. (A2)}$$

The variation in axial force $\Delta N(t)$ can be written as the sum of two contributions (Eq. (A3)), namely the tension changes due to cable length increment and due to lateral displacements, which can be approximated using a Taylor expansion.

$$\Delta N(t) = \frac{EA}{L}\left(\Delta x(t) + \sum_{j=1}^{n}\frac{j^2\pi^2 U_j(t)^2}{4L^2}\right) \qquad \text{Eq. (A3)}$$

Substituting Eq. (A3) into Eq. (A1) and performing a Garlerkin projection on the partial differential equation gives a set of uncoupled Mathieu equations, one for each mode considered. The final equation for mode-*j* is:

$$mL^2\ddot{U}_j + cL^2\dot{U}_j + \frac{j^4\pi^4 EA}{4L^2}{U_j}^3 + j^2\pi^2\left(N + \frac{EA\,\Delta x}{L}\right)U_j = 0 \qquad \text{Eq. (A4)}$$

The transition curves define the boundaries that separate stable from unstable solutions of Eq. (A4). It is possible to derive expressions of these transition curves using the harmonic balance method. This method essentially approximates the solution as a Fourier series (Eq. (A5)) considering N harmonic terms. Substituting Eq. (A5) into Eq. (A4), multiplying the result by the basis $\{\sin(\Omega t), \cos(\Omega t), \ldots, \sin(n\Omega t), \cos(n\Omega t)\}$, integrating over one full cycle and balancing harmonic terms gives a system of equations with the Fourier coefficients Υ_i as the unknowns. Solutions of the system provide the Fourier coefficients that define periodic solutions for Eq. (4). The transition curves are thus defined when the determinant of the coefficient matrix of the system is zero [34].

$$U_j(t) = \sum_{n=0}^{N}\Upsilon_{(2n-1)}\sin(n\Omega t) + \Upsilon_{2n}\cos(n\Omega t) \qquad \text{Eq. (A5)}$$

The analytical expression of the transition curves in the amplitude-frequency plane (A, Ω) is given by Eq. (A6) and Eq. (A7), which is expressed in terms of auxiliary variables defined in

Eq. (A8) to Eq. (A17). Depending on the considered period T (either 2π or 4π) there exist two sets of solutions that correspond respectively to the sum of all even and odd *n* values in Eq. (A5). The number of harmonic terms considered is two ($N = 2$).

$$A(\Omega) = \pm B_1\sqrt{B_2(B_3 \pm \sqrt{B_4})}\ \ for\ T = 2\pi \quad \text{Eq. (A6)}$$

$$A(\Omega) = \pm C_1\sqrt{C_2 \pm \sqrt{C_3}}\ \ for\ T = 4\pi \quad \text{Eq. (A7)}$$

The auxiliary variables are defined below.

$$A_1 = m\,L^2\Omega^2 \quad \text{Eq. (A8)}$$

$$A_2 = N\,j^2\pi^2 \quad \text{Eq. (A9)}$$

$$A_3 = c\,\Omega\,L^2 \quad \text{Eq. (A10)}$$

$$B_1 = \frac{2L}{EAB_2\pi^2 j^2} \quad \text{Eq. (A11)}$$

$$B_2 = 8A_1 - 3A_2 \quad \text{Eq. (A12)}$$

$$B_3 = 2(2A_1 - A_2)(A_3^2 + (A_1 - A_2)(4A_1 - A_2)) \quad \text{Eq. (A13)}$$

$$\begin{gathered} B_4 = 8(2A_1^2 + 2A_1A_2 - A_2^2)A_3^4 \\ +(128A_1^4 - 128A_1^3A_2 + 36A_1^2A_2^2 + 16A_1A_2^3 - 7A_2^4)A_3^2 \\ +(A_1 - A_2)^2(4A_1 - A_2)^4 \end{gathered} \quad \text{Eq. (A14)}$$

$$C_1 = \frac{L\sqrt{2}}{4EA\pi^2 j^2} \quad \text{Eq. (A15)}$$

$$C_2 = 12A_3^2 + (9A_1 - 4A_2)(11A_1 - 12A_2) \quad \text{Eq. (A16)}$$

$$\begin{gathered} C_3 = -432A_3^4 + 8(117A_1^2 - 168A_1A_2 - 176A_2^2)A_3^2 \\ +(13A_1 - 20A_2)(9A_1 - 4A_2)^3 \end{gathered} \quad \text{Eq. (A17)}$$

Acknowledgements

The research presented in this manuscript was possible thanks to the financial support of The Fjord Crossing research program for the Coastal Highway Route E39.

References

[1] Ferjefri E39 summary english jan 2012 http://www.vegvesen.no/vegprosjekter/ferjefriE39/English (accessed 03.10.16).
[2] M.M. Lwin, Floating bridges, in: W.-F. Chen, L. Duan (Eds.), Bridge Engineering Handbook, CRC Press, Boca Raton, 2000.
[3] D. Ahrens, Submerged floating tunnels – A concept whose time has arrived, Tunnelling Undergr. Space Technol. 12 (1997) 317-336. doi: 10.1016/S0886-7798(97)90022-5.

[4] C. Aage, M.M. Bernitsas, H.S. Choi, L. Crudu, A. Incecik, J.J. Murray, The Specialist Committee on Deep Water Mooring. Final report and recommendations to the 22nd ITTC. International Towing Tank Conference, Seoul, 2000.
[5] S. Weller, L. Johanning, P. Davies, Best Practice Report - Mooring of Floating Marine Renewable Energy Devices. Deliverable 3.5.3 from the MERiFIC Project, 2013.
[6] J.L. Lilien, A.P. Da Costa, Vibration amplitudes caused by parametric excitation of cable stayed structures, J. Sound Vibration 174 (1994) 69-90. doi: 10.1006/jsvi.1994.1261.
[7] M.H. El Ouni, N. Ben Kahla, A. Preumont, Numerical and experimental dynamic analysis and control of a cable stayed bridge under parametric excitation, Eng. Struct. 45 (2012) 244–256. doi: 10.1016/j.engstruct.2012.06.018.
[8] A.H. Nayfeh, D.T. Mook, P. Holmes, Nonlinear Oscillations, Wiley-VCH and Publishing House, Weinheim, Germany, 2004. doi: 10.1115/1.3153771.
[9] E.S. Caetano, Cable Vibrations in Cable-Stayed Bridges, International Association for Bridge and Structural Engineering, Zürich, Switzerland, 2007.
[10] I.K. Chatjigeorgiou, N.I. Xiros, S.A. Mavrakos, Coupling contributions and effect of Mathieu instabilities in the dynamic behaviour of vertical elastic cables and risers, WSEAS/IASME International Conference on Fluid Mechanics, Corfu, 2004.
[11] R.A. Ibrahim, Nonlinear vibrations of suspended cables—part III: Random excitation and interaction with fluid flow, Appl. Mech. Rev. 57 (2004) 515-549. doi: 10.1115/1.1804541.
[12] V.J. Papazoglou, S.A. Mavrakos, M.S. Triantafyllou, Non-linear cable response and model testing in water, J. Sound Vibration 140 (1990) 103-l 15. doi: 10.1016/0022-460X(90)90909-J.
[13] M.H. Patel, H.I. Park, Dynamics of tension leg platform tethers at low tension. part I - Mathieu stability at large parameters, Mar. Struct. 4 (1991) 257-273. doi: 10.1016/0951-8339(91)90004-U.
[14] S. Chandrasekaran, N.R. Chandak, G. Anupam, Stability analysis of TLP tethers, Ocean Eng. 33 (2006) 471–482. doi: 10.1016/j.oceaneng.2005.04.015.
[15] I.K. Chatjigeorgiou, S.A. Mavrakos, Nonlinear resonances of parametrically excited risers-numerical and analytic investigation for $\Omega = 2\omega_1$, Comput. Struct. 83 (2005) 560–573. doi: 10.1016/j.compstruc.2004.11.009.
[16] G.R. Franzini, C.E.N. Mazzilli, Non-linear reduced-order model for parametric excitation analysis of an immersed vertical slender rod, Int. J. Non-Linear Mech. 80 (2016) 29–39. doi: 10.1016/j.ijnonlinmec.2015.09.019.
[17] S. Lei, W. Zhang, J. Lin, Q. Yue, D. Kennedy, F.W. Williams, Frequency domain response of a parametrically excited riser under random wave forces, J. Sound Vibration 333 (2014) 485–498. doi: 10.1016/j.jsv.2013.09.025.
[18] N. Srinil, G. Rega, The effects of kinematic condensation on internally resonant forced vibrations of shallow horizontal cables, Int. J. Non-Linear Mech. 42 (2007) 180–195. doi: 10.1016/j.ijnonlinmec.2006.09.005.
[19] G. Rega, N. Srinil, R. Alaggio, Experimental and numerical studies of inclined cables: free and parametrically-forced vibrations, J. Theor. Appl. Mech. 46 (2008) 621-640.
[20] N. Srinil, G. Rega, S. Chucheepsakul, Three-dimensional non-linear coupling and dynamic tension in the large-amplitude free vibrations of arbitrarily sagged cables, J. Sound Vibration 269 (2004) 823–852. doi: 10.1016/S0022-460X(03)00137-8.
[21] H. Yang, F. Xiao, P. Xu, Parametric instability prediction in a top-tensioned riser in irregular waves, Ocean Eng. 70 (2013) 39–50. doi: 10.1016/j.oceaneng.2013.05.002.

[22] I.K. Chatjigeorgiou, On the parametric excitation of vertical elastic slender structures and the effect of damping in marine applications, Appl. Ocean Res. 26 (2004) 23–33. doi: 10.1016/j.apor.2004.08.001.
[23] J.A.P. Aranha, M.O. Pinto, Dynamic tension in risers and mooring lines: an algebraic approximation for harmonic excitation, Appl. Ocean Res. 23 (2001) 63-81. doi: 10.1016/S0141-1187(01)00008-6.
[24] J.A.P. Aranha, M.O. Pinto, A.J.P. Leite, Dynamic tension of cables in a random sea: analytic approximation for the envelope probability density function, Appl. Ocean. Res. 23 (2001) 93-101. doi: 10.1016/S0141-1187(01)00010-4.
[25] Det Norske Veritas, Guideline for Offshore Structural Reliability Analysis – Examples for Tension Leg Platforms, Report No. 95-3198, 1995.
[26] Det Norske Veritas, Fatigue Design of Offshore Steel Structures. Recommended Practice DNV-RP-C203, 2011.
[27] ABAQUS, Analysis User's Manual, Dassault Systèmes, Providence, 2011.
[28] M.M. Gadagi, H. Benaroya, Dynamic response of an axially loaded tendon of a tension leg platform, J. Sound Vibration 293 (2006) 38–58. doi: 10.1016/j.jsv.2005.09.027.
[29] Det Norske Veritas SA, Recommended Practice DNV-RP-C205: Environmental Conditions and Environmental Loads, 2014.
[30] C. Webster, Mooring-induced damping, Ocean Eng. 22 (1995) 571-591. doi: 10.1016/0029-8018(94)00027-5.
[31] W..-C. Xie, Dynamic Stability of Structures, Cambridge University Press, Cambridge, United Kingdom, 2006.
[32] R.S. Zounes, R.H. Rand, Transition curves for the quasi-periodic Mathieu equation, SIAM J. Appl. Math. 58 (1998) 1094-1115. doi: 10.1137/S0036139996303877.
[33] C.T. Georgakis, C.A. Taylor, Nonlinear dynamics of cable stays. part 1: Sinusoidal cable support excitation, J. Sound Vibration 281 (2005) 537–564. doi: 10.1016/j.jsv.2004.01.022.
[34] D. Cantero, A. Rønnquist, A. Naess, Recent studies of parametrically excited mooring cables for submerged floating tunnels, Procedia Eng. 166 (2016) 99-106. doi: 10.1016/j.proeng.2016.11.571